B. TECH. PROJECT REPORT

ON

AUTOMATED SCREENING OF SLEEP APNEA FROM ECG SIGNALS USING DIGITAL TAYLOR-FOURIER TRANSFORM

BY

Anmol Mansingh (150002008)
Banka Nithin (150002010)

DISCIPLINE OF ELECTRICAL ENGINEERING

INDIAN INSTITUTE OF TECHNOLOGY INDORE

December 2018

AUTOMATED SCREENING OF SLEEP APNEA FROM ECG SIGNALS USING DIGITAL TAYLOR-FOURIER TRANSFORM

A PROJECT REPORT

Submitted in partial fulfillment of the requirements for the award of the degrees

of

BACHELOR OF TECHNOLOGY
in
ELECTRICAL ENGINEERING

Submitted by:
Anmol Mansingh (150002008)
Banka Nithin (150002010)

Guided by:
Dr. Ram Bilas Pachori
Professor, Electrical Engineering
IIT Indore, Indore, India

INDIAN INSTITUTE OF TECHNOLOGY INDORE
December 2018

CANDIDATES' DECLARATION

We hereby declare that the project entitled **"Automated screening of sleep apnea from ECG signals using digital Taylor-Fourier transform"** submitted in partial fulfillment for the award of the degree of Bachelor of Technology in 'Electrical Engineering' completed under the supervision of **Dr. Ram Bilas Pachori, Professor, Discipline of Electrical Engineering, IIT Indore, Indore, India** is an authentic work.

Further, we declare that we have not submitted this work for the award of any other degree elsewhere.

Anmol Mansingh **Banka Nithin**

CERTIFICATE by BTP Guide

It is certified that the above statement made by the students is correct to the best of my knowledge.

Dr. Ram Bilas Pachori

Professor, Discipline of Electrical Engineering

IIT Indore, Indore, India

Preface

This report on **"Automated screening of sleep apnea from ECG signals using digital Taylor-Fourier transform"** is prepared under the guidance of Dr. Ram Bilas Pachori, Professor, Electrical Engineering, IIT Indore.

Through our report we have developed a novel method for effective detection of obstructive sleep apnea (OSA) from single-lead electrocardiogram (ECG) signals using the digital Taylor-Fourier transform (DTFT). This method is computationally less intensive than its predecessors while maintaining high accuracy. Our methodology, when implemented in real-life situations, will save on time without compromising on accuracy, potentially saving many precious lives.

We have tried to the best of our abilities and knowledge to explain the content in a lucid manner.

Anmol Mansingh
B.Tech. IV Year
Discipline of Electrical Engineering
IIT Indore

Banka Nithin
B.Tech. IV Year
Discipline of Electrical Engineering
IIT Indore

Acknowledgement

We wish to thank Dr. Ram Bilas Pachori for his kind support and valuable guidance throughout the course of the project.

We also thank PhD scholar Mr. Vipin Gupta for his assistance.

We would also like to thank our families and friends for constantly supporting us and believing in us.

It is with their help and support, due to which we were able to complete the project and prepare this report.

Anmol Mansingh
B.Tech. IV Year
Discipline of Electrical Engineering
IIT Indore

Banka Nithin
B.Tech. IV Year
Discipline of Electrical Engineering
IIT Indore

Abstract

Obstructive sleep apnea (OSA) is one of the most prevalent respiratory disorders in humans, and often leads to cardiovascular complications in the long run. Hence, it is essential to develop techniques that effectively detect the condition, while keeping operating time and costs to a minimum. Methods using the single-lead electrocardiogram (ECG) signals have proven to be an economical and computationally feasible option. In this report, a new methodology based on the digital Taylor-Fourier transform (DTFT) has been developed for sleep apnea detection and classification from single-lead ECG signals. In this method, a DTFT matrix (similar to the twiddle factor matrix) has been used to extract features from the apnea and non-apnea ECG signals. The signals are decomposed into various oscillatory modes, represented by the coefficients obtained after the DTFT is applied. The DTFT enables us to evaluate multiple frames at a time in the process of obtaining these coefficients. The magnitude of the features is then evaluated from the spectral coefficients. The support vector machine (SVM) classifier, along with the radial basis function (RBF) kernel is used for the purpose of classification. The proposed approach yielded a maximum classification accuracy of 92.41% using the Physionet-Apnea ECG database.

Table of Contents

List of Figures

List of Table

Chapter 1

Introduction

1.1 Sleep apnea

The sleep apnea is a very common respiratory disorder that occurs during sleep [1]. Obstructive sleep apnea (OSA) is a form of apnea where the upper airway becomes blocked repeatedly during sleep, reducing or completely stopping airflow [2]. If the brain does not send the signals needed to breathe, the condition is called central sleep apnea (CSA). There is a third category of sleep apnea named mixed sleep apnea (MSA). Specifically, an absence of airflow for at least 10 sec is classified as an obstructive apnea episode [3]. Although the OSA is a treatable condition, it often goes undetected, which can be inferred from the fact that around 85% of patients with clinically significant apnea have never been diagnosed [4]. Sleep apnea occurs in all age groups and both sexes, but is more common in men. The frequent interruptions of deep, restorative sleep due to OSA often lead to early morning headaches and excessive daytime sleepiness. Early detection and treatment of OSA is vital as it may lead to various cardiovascular complications such as an irregular heartbeat, heart attacks, and strokes [5].

1.2 Purpose of this work

As discussed in the previous section, OSA is a very common disorder, and there are high chances it might go undetected in most adults. Late detection allows for the onset of various cardiovascular conditions, which could have otherwise been prevented if a more proactive approach was taken [5]. To this end, there are many techniques which allow for early detection of sleep apnea. For a very long time, the most common approach for this has been polysomnography (PSG) [3]. This technique requires many channels, which in turn means more electrodes and sensors attached to the patient's body [6]. This means that, along with increased operational costs and time, the patient's sleep is degraded as well. Also, there is scope for error as it is reliant on the observational skills of the physicians monitoring the patient, which is subjective.

This lead research on sleep apnea detection to look towards single-lead electrocardiogram (ECG) signals [7]. Not only is this means of collecting data cheaper [8], it reduces discomfort on the patient due to less number of sensors, ensuring better sleep and hence more reliable data. Many

techniques for detection of OSA using the single-lead ECG signals are available in the literature. Methods [9], [10], [11] and [12] directly use the single-lead ECG signals, although [13] and [14] rely on the heart-rate variability (HRV) and ECG-derived respiration (EDR) signals that accompany the single-lead ECG signals.

In [15], a new method to analyze signals using dynamic phasors was introduced, which then led to the formulation of the digital Taylor-Fourier transform (DTFT) [16]. When applied on a signal, it generates coefficients that give information about the frequency spectrum at multiples of a fundamental frequency. It gives more information than the standard discrete Fourier Transform (DFT) as it works on the dynamic phasor assumption, and hence contains more coefficients. Coming to the problem at hand, as the annotations are given for every minute, the ECG signal is split into non-overlapping frames. Compared to the previous methods discussed earlier, the DTFT is computationally feasible [17] as it can be applied to multiple frames at a time. In our proposed method, we explore DTFT for the application of sleep apnea detection using ECG signals.

1.3 Proposed method

In this work, initially the ECG signals (which are of 3 types, A, B and C based on the duration of apnea) are segmented into one-minute frames as the apnea annotations are given for one-minute durations. The classification of each segment as apnea or non-apnea are performed using features extracted from the operation of the DTFT. The DTFT is implemented as a matrix, which is unable to cover the entire minute duration on its own due to size constraints. Hence, each one minute signal is further divided into sub-frames and coefficients are obtained from each sub-frame. For classification, the magnitude of these coefficients is taken as the features. To get common features for the one minute duration, the sub-frame features are averaged throughout each minute. These features correspond to different oscillating frequencies present in the signal. A feature matrix is generated for with features for each minute acting as feature vectors. It is given as the input to the classifier, which classifies them as apnea or non-apnea. The block diagram of the proposed method is illustrated in Fig. 1.1.

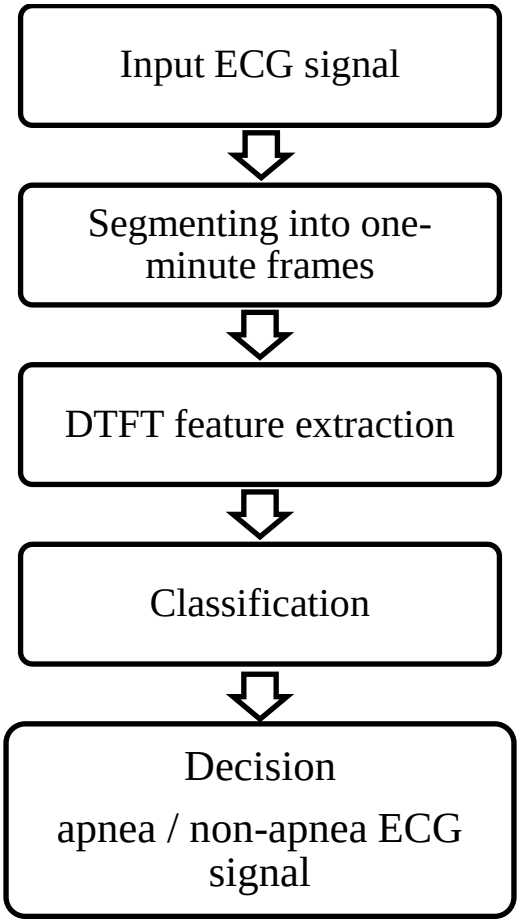

Fig. 1.1: Block diagram of the proposed method

Chapter 2

ECG database

The ECG database used in this work is a publicly available apnea ECG database [18] obtained from https://physionet.org/physiobank/database/apnea-ecg/. The data consists of 70 records of ECG signals, which are divided into 35 training and 35 testing sets. All the recordings in the database vary from 7 - 10 hours each. Each recording includes a continuous digitized ECG signal, a set of apnea annotations for every minute derived by human experts on the basis of simultaneously recorded respiration and related signals. All the recordings are 16 bits per sample, least significant byte first in each pair, 100 samples per second, nominally 200 analog/digital (A/D) units per millivolt.

2.1 Data acquisition

Each of the 35 ECG recordings is divided into one-minute signals. The annotations to these one-minute signals are made accordingly. These one-minute signals consists of 6000 samples each (number of samples = sampling rate (samples/sec.)×time (sec.) i.e. 100×60 = 6000 samples). After dividing them so, we got 6514 apnea and 10531 non-apnea one-minute signals. The further processes in our work are based on these signals. These signals have been adjusted according to their gain as mentioned in the database. They have a nominal gain of 200 A/D units per millivolt. Fig 2.1 and 2.2 represent one-minute duration ECG signals for a subject who does not have apnea and a patient who has apnea, respectively.

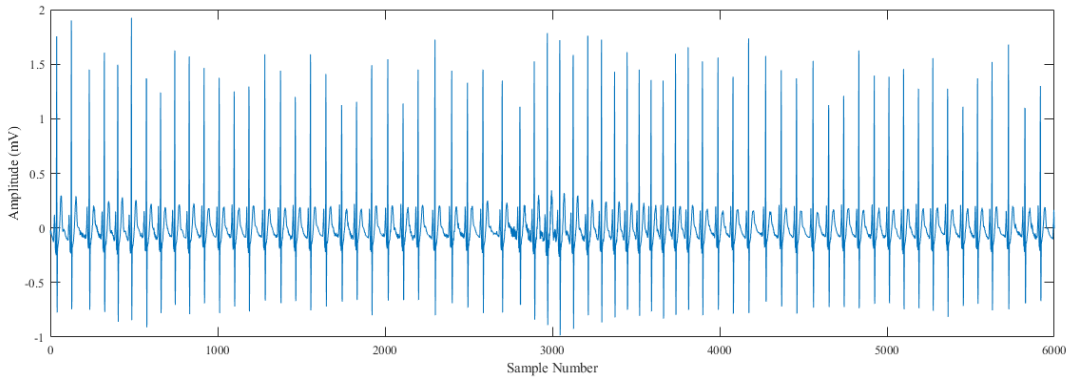

Fig 2.1: Non-apnea ECG signal recorded from a subject

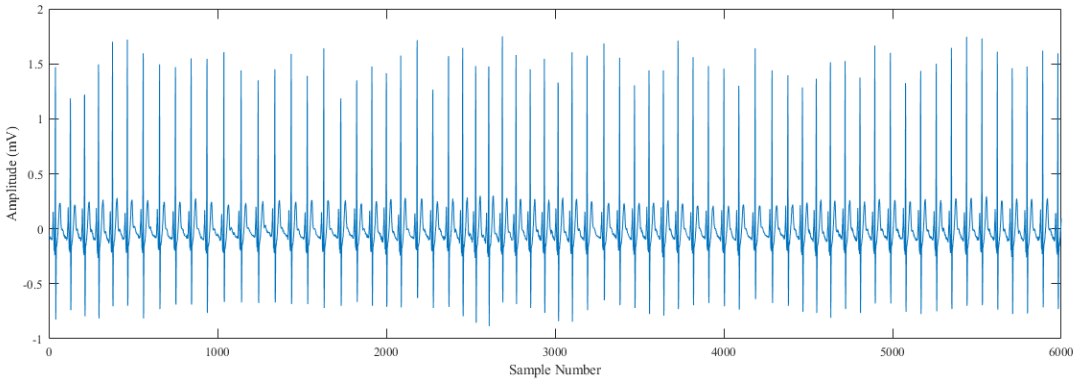

Fig 2.2: Apnea ECG signal recorded from a patient

Chapter 3

Digital Taylor-Fourier transform

The DTFT [16] is an extension of the discrete Fourier Transform (DFT), where the phasor has been assumed to be dynamic and its amplitude represented by a time-varying Taylor series. It is primarily dependent on two parameters: the fundamental frequency (f_0) and the order of the dynamic phasor amplitude (K).

3.1 Chronology

The problem of signal decomposition has been integral to signal processing since time immemorial, with various methods being proposed and several improvements made over time. Closely related to this is the problem of harmonic estimation. Existing harmonic techniques have been helpful to solve a lot of problems that arise from several areas, some of which have been given in [19], [20] and [21]. The familiar techniques of DFT and the computationally-superior fast Fourier transform (FFT) have been very effective in static harmonic estimation. However, it is well known that, in practice, signals do not accomplish this ideal property. Using methods suited for static estimation, such as the DFT, to estimate the Fourier coefficients of these signals would then result in the following anomalies: 1) spectral leakage and 2) harmonic interference [22]. To account for these discrepancies, a new signal model, based on the concept of dynamic phasors is presented in [15]. In [16], this signal model is realized via the Taylor – Fourier transform (TFT).

3.2 Methodology

Since its conception in [23], the phasor has essentially been considered as a steady-state concept. Up to now, this assumption is the basis for most of the algorithms for phasor estimation. Existing estimation methods assume that the analyzed signal is periodic, which implies constant fundamental frequency and Fourier coefficients (amplitude and phase) over the entire observation window. This adds to the static phasor assumption. Taking this assumption, the DFT is used to get the spectral coefficients, which are constants.

The static phasor model for a sinusoidal signal $s(t)$ with fundamental frequency f_0, amplitude a_0 and initial phase ϕ_0 is given as:

$$s(t) = a_0 \cos\left(2\pi f_0 t + \phi_0\right), \quad -\frac{T}{2} \leq t \leq \frac{T}{2}, \tag{3.1}$$

where T is the time period of the signal.

In a signal with multiple harmonics to be estimated, the static model is given as:

$$x_p(t) = \sum_{h=-H}^{H} d_h \, e^{j2\pi h f_0 t} \tag{3.2}$$

Where H is the number of harmonics present in the signal, f_0 is the fundamental frequency, and d_h is the amplitude of each harmonic.

The constant coefficients fail to capture the oscillatory nature of the real-life signals at each harmonic. Also, they are unable to convey frequency information in the vicinity of the harmonics. To rectify this, a new approach was presented in [15]. This work relaxes the static phasor assumption to a dynamic one, i.e., the dynamic phasor $p(t)$, which is one complex time function with movement freedom. The dynamic phasor model is given as:

$$\begin{aligned} s(t) &= \tfrac{1}{2}\left(p(t)e^{j2\pi f_0 t} + \bar{p}(t)e^{-j2\pi f_0 t}\right) \\ &= Re\left\{p(t)e^{j2\pi f_0 t}\right\}, \quad -\frac{T}{2} \leq t \leq \frac{T}{2}, \end{aligned} \tag{3.3}$$

where $p(t) = a(t)e^{j\phi(t)}$. The $a(t)$ and $\phi(t)$ are the time-varying amplitude and phase components of the phasor respectively.

It can also be written as follows:

$$x(t) = \sum_{h=-H}^{H} d_h(t) \, e^{j2\pi h f_0 t} \tag{3.4}$$

The phasor $p(t)$ in **(3.3)** is then approximated by a k^{th}-order Taylor polynomial, as shown below:

$$p(t) = p(0) + p'(0)t + p''(0)\frac{t^2}{2!} + \cdots + p^k(0)\frac{t^k}{k!} \quad \textbf{(3.5)}$$
$$for \ \ -\frac{T}{2} \le t \le \frac{T}{2}$$

Comparing **(3.4)** and **(3.5)**, we can see that for N signal points, the number of unknown coefficients will be $(2H+1)(K+1)$. For these number of signal points, the maximum number of equations to solve would be $N(K+1)$.

Similar to the traditional Fourier matrix with twiddle factors w_N^{kn}, we can have

$$\boldsymbol{W}_N = \begin{pmatrix} 1 & 1 & 1 & \cdots & 1 \\ 1 & w_n & w_n^2 & \cdots & w_N^{(N-1)} \\ 1 & w_n^2 & w_n^4 & \cdots & w_N^{2(N-1)} \\ \vdots & \vdots & \vdots & \ddots & \vdots \\ 1 & w_N^{(N-1)} & w_N^{2(N-1)} & \cdots & w_n^{(N-1)^2} \end{pmatrix} \quad \textbf{(3.6)}$$

which is of dimension $N \times N$ for N signal points, we now need a $N(K+1) \times N(K+1)$ matrix, which is named the Taylor-Fourier matrix, which is given in [24] as

$$\hat{x}_{CN} = \boldsymbol{B}_{CN}\hat{\boldsymbol{\xi}}_{CN} = \begin{pmatrix} \boldsymbol{I}_{CN}\begin{pmatrix} \boldsymbol{W}_N \\ \boldsymbol{W}_N \\ \vdots \\ \boldsymbol{W}_N \end{pmatrix} & \boldsymbol{T}_{CN}\begin{pmatrix} \boldsymbol{W}_N \\ \boldsymbol{W}_N \\ \vdots \\ \boldsymbol{W}_N \end{pmatrix} & \cdots & \frac{1}{k!}\boldsymbol{T}_{CN}^K\begin{pmatrix} \boldsymbol{W}_N \\ \boldsymbol{W}_N \\ \vdots \\ \boldsymbol{W}_N \end{pmatrix} \end{pmatrix} \begin{pmatrix} \hat{\boldsymbol{\xi}}_N \\ \hat{\dot{\boldsymbol{\xi}}}_N \\ \vdots \\ \widehat{\boldsymbol{\xi}^{\boldsymbol{K}}}_N \end{pmatrix} \quad \textbf{(3.7)}$$

This matrix has $C = K+1$ vertical matrices, each one formed by C Fourier matrices $\boldsymbol{W}_N$, one below the other, with harmonic vectors of length $L = C \times N$, which will modulate the Taylor terms in the C diagonal matrices $\frac{1}{k!}T_{CN}^k, k = 0, \ldots, K$. The diagonal matrix T_{CN}, has in its diagonal the following sequence $\boldsymbol{l} = \frac{[-L_h \ -L_h+1 \ \ldots \ L_h]}{Nf_0}$; where $L_h = (L-1)/2$. Note that for odd lengths, the vector $\boldsymbol{l}$ contains integers, and for even ones, halves. The vector $\hat{\boldsymbol{\xi}}_{CN}$ contains up to the *K*th harmonic phasor derivative.

Then, the DTFT is given by the least-square solution:

$$\hat{\boldsymbol{\xi}}_{CN} = (\boldsymbol{B}_{CN}^{H}\boldsymbol{B}_{CN})^{-1}\,\boldsymbol{B}_{CN}^{H}\,x_{CN} \tag{3.8}$$

Where $(\boldsymbol{B}_{CN}^{H}\boldsymbol{B}_{CN})^{-1}\boldsymbol{B}_{CN}^{H}$ is called the pseudoinverse matrix of $\boldsymbol{B}_{CN}$ and denoted as $\boldsymbol{B}^{\dagger}$.

3.3 Spectral coefficients

In **(3.8)**, the coefficients $\hat{\boldsymbol{\xi}}_{CN}$ are shown to have been obtained by applying $\boldsymbol{B}^{\dagger}$ on the input signal x_{CN}. In order to generate coefficients which relate to multiples of our fundamental frequency, we define N as the samples per fundamental cycle ($T = 1/f_0$). Then, each row of the matrix $\boldsymbol{W}_N$ will correspond to frequencies that are multiples of the fundamental frequency, and will cover frequencies upto f = f_s, where f_s is the sampling frequency. Drawing parallels with the DFT, we see that for K = 0 (C = K+1 = 1), the pseudoinverse matrix $\boldsymbol{B}^{\dagger}$ gives the DFT. This is justified as for K = 0, as we are working under the static phasor assumption. Hence, it can be said that the DTFT is an extension of the DFT. Further, it is given in [16] that

$$\hat{\boldsymbol{\xi}}_{(k,h)} \simeq \frac{T_s^k}{k!}\left(\frac{d^k d_h(t)}{dt^k}\,\middle|\, t = 0\right) \tag{3.9}$$

which shows that the DTFT coefficients are related to the dynamic phasor coefficients and separated only by a constant factor of $\frac{T_s^k}{k!}$ (where T_s = sampling period, k = Taylor polynomial order). In our analysis of coefficients, we consider only half of the coefficients in each cycle of N coefficients as they cover frequencies upto half of the sampling frequency, $\frac{f_s}{2}$, which is the maximum possible frequency present in the signal according to the Nyquist theorem.

3.4 DTFT filters

According to [16], each row of the DTFT matrix corresponds to the time-reversed impulse responses of the DTFT filters. As discussed above, each row has filters centered at multiples of the fundamental frequency. Increasing the order K leads to change in shape of the filters, specifically flatter pass-bands and lower sidelobes. Decreasing the fundamental frequency allows us to capture more spectral information, and hence require low-bandwidth filters. These changes are illustrated in the next chapter. The filter bank can then be used for obtaining sub-band signals

by convolution of desired filter with the signal. For illustrative purposes, the DTFT filters are plotted in the Fig. 3.1 for f_0 = 5 Hz and K = 5.

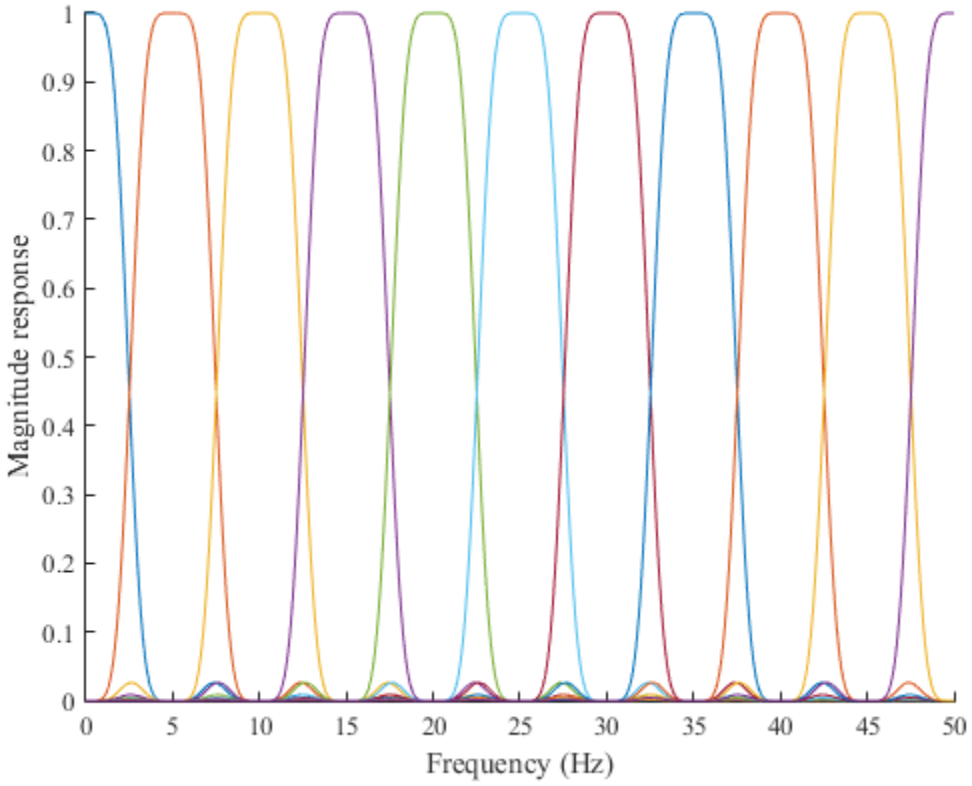

Fig. 3.1: Zero order DTFT filter bank

Chapter 4

Feature extraction

Features are one or more set of values that describe characteristic properties of the signals in machine learning (ML) problems. ML problems are categorized into many types. In this work, the ML problem we deal with is a classification problem and falls under supervised learning. A Supervised learning is a process of learning where the input and output are provided explicitly. Classification, as the name suggests, is a process of classifying things into their respective classes using the data provided (explained in chapter 5).

In this chapter, we focus on how we have extracted the features and the reason for selecting those features.

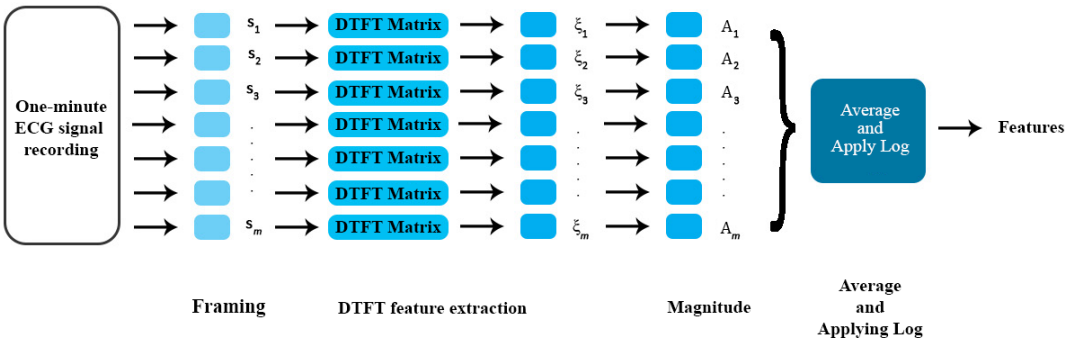

Fig. 4.1 - Feature extraction

4.1 DTFT feature extraction

DTFT is an intuitive way of looking at the ECG signals. DTFT approach attempts to approximate the time dependent frequency components. As mentioned in chapter 3, it assumes that the Fourier coefficients are not just constants but they are polynomials in time 't'. This gives us more insights about the signals.

Depending on how well the DTFT filter banks can spread over and the amount of overlap between filters, we have decided an optimal filter which covers maximum of the frequency band without compromising on the amount of overlap. Fig. 4.2 shows the effect of f_0 and C = (K+1, where K is order of Taylor polynomial) on the filter responses.

For feature extraction, the one-minute signals are divided into sub-frames $\boldsymbol{s_m}$ (where m = 1 to $\frac{6000}{N}$) as shown in Fig. 4.1 of suitable length depending on the size of $\boldsymbol{B}^{\dagger}$. These sub-frames are multiplied with $\boldsymbol{B}^{\dagger}$ to get DTFT Coefficients. Choosing a fundamental frequency of f_0 Hz, $N = \frac{f_s}{f_1}$, care is taken that N will be an integer, divides 6000, and f_s evenly and the order of Taylor polynomial is taken as $K = 2$. Then $\boldsymbol{B}^{\dagger}$ has $N(K+1) \times N(K+1)$ size. The frames of length 6000 samples are divided into $\frac{6000}{N(K+1)}$ sub-frames of N samples each. These sub-frames are multiplied individually with $\boldsymbol{B}^{\dagger}$ to get $N(K+1) \times 1$ coefficient vector ($\hat{\boldsymbol{\xi}}$) as in equation 4.1.1. The first N coefficients correspond to the zeroth order of Taylor approximating polynomial, the second to the first and the third to the second order. These coefficients give us information about the frequencies from 0 – 100 Hz with f_0 Hz separation.

From **(3.8)**, we have

$$\hat{\boldsymbol{\xi}}_{\boldsymbol{m}} = \boldsymbol{B}^{\dagger}.\boldsymbol{s_m}, \tag{4.1}$$

where m = 1 to $\frac{6000}{N(K+1)}$, $\boldsymbol{s_m}$ is a sub-frame, $\hat{\boldsymbol{\xi}}_{\boldsymbol{m}}$ is a vector and **(4.1)** can also be written as,

$$\hat{\boldsymbol{\xi}}_{\boldsymbol{m}} = [\boldsymbol{\xi_{m,1}}, \boldsymbol{\xi_{m,2}}, \boldsymbol{\xi_{m,3}}, \cdots, \boldsymbol{\xi_{m,N(K+1)}}] \tag{4.2}$$

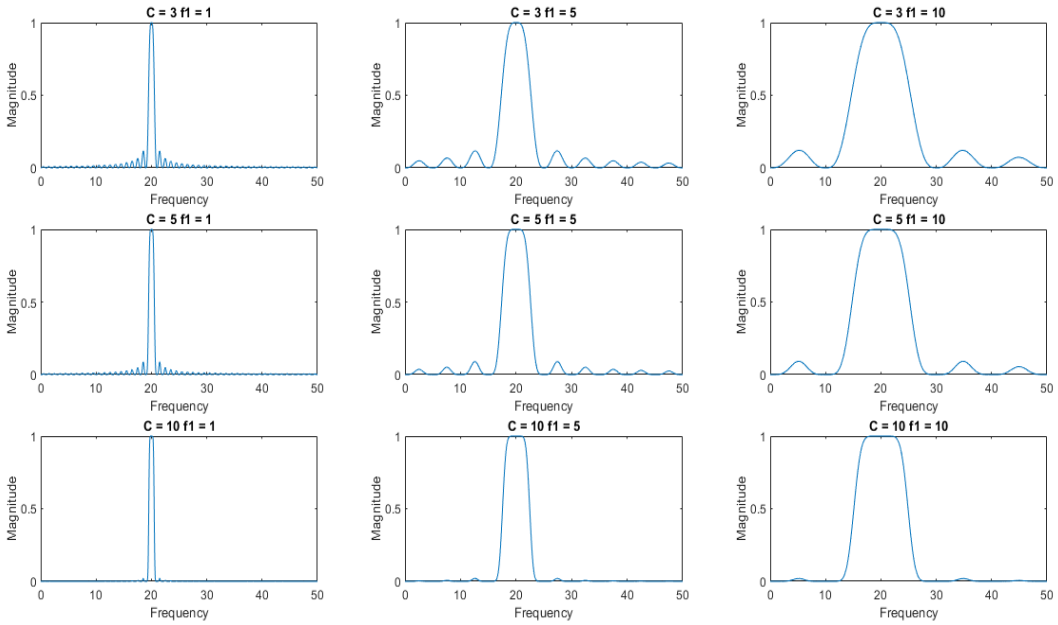

Fig. 4.2: Effect of changing 'C' and 'f_0' on DTFT Filter at 20 Hz frequency.

We have considered those coefficients that give the spectral information present in the 0-50 Hz frequency band, which means we have considered first $\frac{N}{2}+1$ coefficients from every order starting from zeroth order to till K^{th} order. Since the coefficients are complex, magnitude of individual coefficients is taken which leads us to a set $\boldsymbol{A_m}$ corresponding to m^{th} sub-frame. Likewise, we can obtain features for all the $\frac{6000}{N(K+1)}$ sub-frames. Then, an average of coefficients is taken as shown in **(4.5)** to form $\boldsymbol{F}$ as shown in **(4.6)**. Now, features resulted from coefficients corresponding to those 0-50 Hz band as mentioned above are chosen. This gives $(\mathrm{K}+1)(\frac{N}{2}+1)$ features for a one-minute signal. All these features for one-minute signals put together gives us a dataset.

$$\boldsymbol{A_m} = [\boldsymbol{a_{m,1}}, \boldsymbol{a_{m,2}}, \boldsymbol{a_{m,3}}, \dots., \boldsymbol{a_{m,N(K+1)}}], \quad \textbf{(4.3)}$$

Where $\boldsymbol{m}$ = 1 to $\frac{6000}{N(K+1)}$,

$$\boldsymbol{a_{m,j}} = |\boldsymbol{\xi_{m,j}}|, \quad \textbf{(4.4)}$$

Where $\boldsymbol{j}$ = 1 to $N(K+1)$,

$$\boldsymbol{f_j} = \frac{1}{\left(\frac{6000}{N}\right)} \sum_{i=1}^{\frac{6000}{N\times(K+1)}} \boldsymbol{a_{mj}}, \quad \textbf{(4.5)}$$

Where $\boldsymbol{j}$ = 1 to $N(K+1)$,

$$\boldsymbol{F} = [\boldsymbol{f_1}, \boldsymbol{f_2}, \dots, \boldsymbol{f_p}], \quad \textbf{(4.6)}$$

Where $\boldsymbol{p}$ = $N(K+1)$.

4.2 Logarithmic transformation

Before using these coefficients as features for classification, studying the distribution of the coefficients is very important. We have used histograms to study the distribution of these coefficients.

The logarithm (ln) transformation has been used on the features, and its use is found to have increased the classification accuracy. The histograms plotted below in Fig 4.3 show the effect of this transformation.

(a)

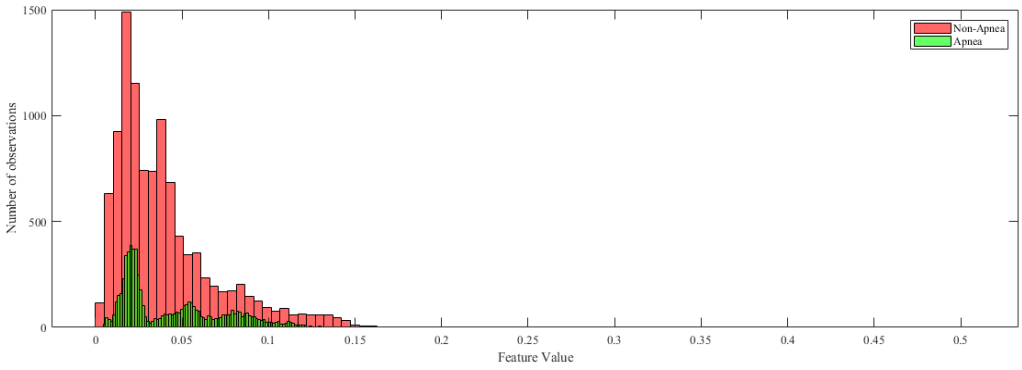

(b)

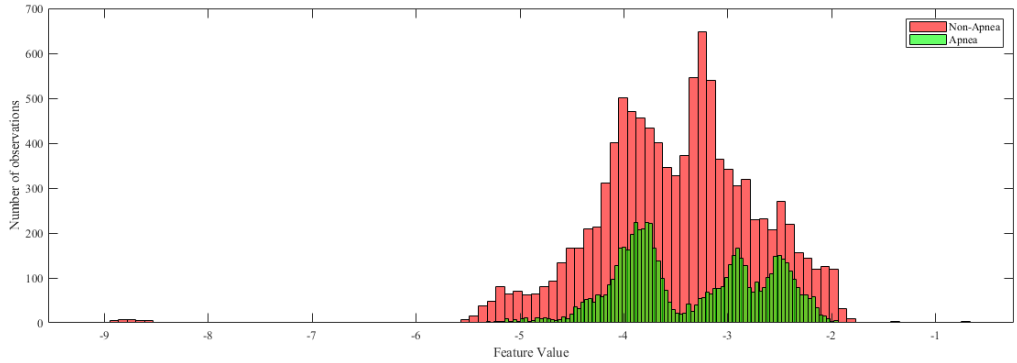

Fig. 4.3: Effect of logarithmic transformation on a feature. (a) Data distribution before applying logarithmic transforamtion. (b) Data distribution after applying logarithmic transformation.

Chapter 5

Classification

Classification is the process of deciding to which class an observation belongs to given that we have prior knowledge of different observations and their groups/classes they belong to.

An algorithm which performs the task of classification is called a classifier. A classifier has to be trained with the observations given beforehand to let it make a decision criteria for the groups/classes.

5.1 Support vector machine classifier

The support vector machine, abbreviated and popularly known in ML domain as SVM, was invented by Corinna Cortes and Vladimir N.Vapnik [25]. The SVM is a supervised learning algorithm that analyzes the training data to decide so called hyperplane which identifies the groups.

We have used Matlab as a tool for applying ML algorithms and training them. We have opted for the SVM with a radial basis function (RBF) as a kernel. In ML, kernel methods are a class of algorithms for pattern analysis. The general task of pattern analysis is to find and study general types of relations (for example clusters, rankings, principal components, correlations, classifications) in datasets. In its simplest form, the kernel trick means transforming data into another dimension that has a clear dividing margin between classes of data.

The classes or groups are apnea and non-apnea, that is we have a binary situation: yes or no classification of such data is called binary classification. SVMs are inherently binary classifiers. However, methods have been developed to use it for multiclass classification (when the number of classes are more than 2).

5.2 k-fold cross-validation

In k-fold cross-validation technique, the dataset is divided into k parts randomly, the model is trained on k-1 parts and tested on k^{th} partition [26]. This is done k-1 times using all the k parts individually, where each of those k parts becomes a test set in every iteration. The accuracy is

taken for all the k-1 validations and averaged to get k-fold cross-validation accuracy of the model. k-fold cross-validation protects the model against biasing to some extent.

5.3 Accuracy

Accuracy of a model is a very important measure to determine its quality and performance. In general, it is defined as [27]

$$\text{Accuracy} = \frac{\text{Number of correct predictions}}{\text{Total number of predictions}} \times 100 \quad \textbf{(5.1)}$$

For a binary classification, we define apnea as the positive class and non-apnea as the negative class.

Let us define the following terms,

True positive (TP): The observations which belong to a positive class and are predicted as belonging to positive class are called TP cases.

True negative (TN): The observations which belong to a negative class and are predicted as belonging to negative class are called TN cases.

False positive (FP): The observations which belong to a positive class and are predicted as belonging to negative class are called FP cases.

False negative (FN): The observations which belong to a negative class and are predicted as belonging to positive class are called FN cases.

A 2×2 matrix is also developed with these values, called the confusion matrix. Fig. 5.1 shows how a confusion matrix looks like.

Accuracy for binary classes can also be defined as:

$$\text{Accuracy} = \frac{\text{TP}+\text{TN}}{\text{TP}+\text{FP}+\text{TN}+\text{FN}} \times 100 \quad \textbf{(5.2)}$$

Sensitivity: It is a measure of the proportion of actual positives that are correctly identified as such.

$$\text{Sensitivity} = \frac{\text{TP}}{\text{TP+FN}} \times 100 \quad \textbf{(5.3)}$$

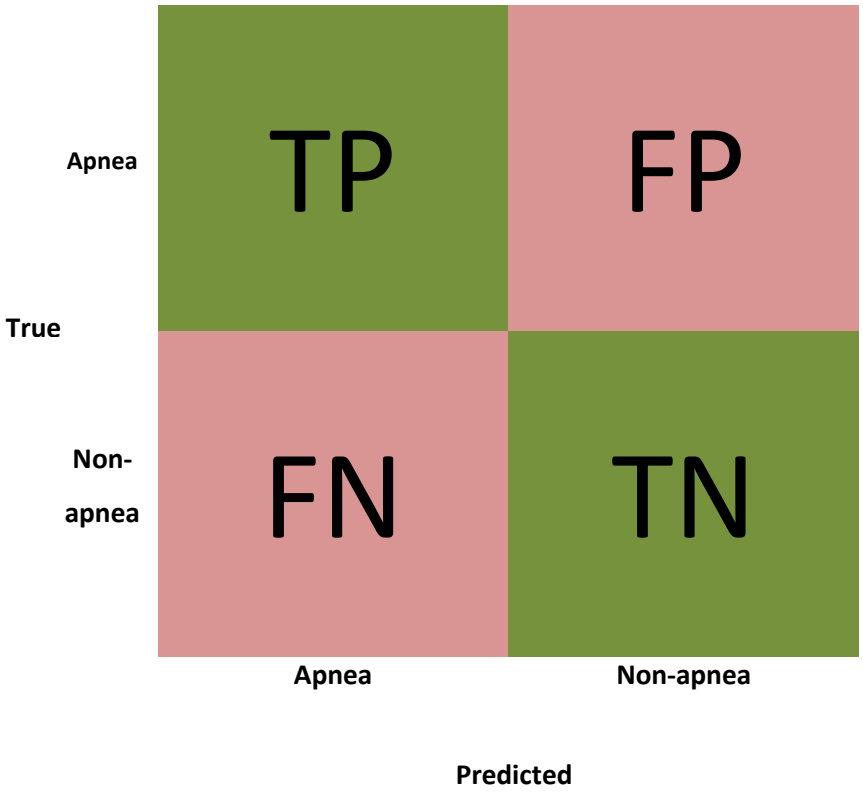

Fig. 5.1: General confusion matrix

Specificity: It is a measure of the proportion of actual negatives that are correctly identified as such.

$$\text{Specificity} = \frac{\text{TN}}{\text{TN+FP}} \times 100 \quad \textbf{(5.4)}$$

Chapter 6

Results and discussions

The Physionet apnea-ECG database gave 17045 observations, out of which 6514 are apnea and 10531 are non-apnea observations. Out of these few were found to be insignificant because the signals were zero for the entire one-minute duration. Removing them, we ended up with 17028 observations consisting of 6513 apnea events and 10515 non-apnea events. As shown in Fig. 4.2 we have checked for the effect of f_0 and C on the filter bank response. From studying them, we have selected the values $C = (K+1) = 3$ and $f_0 = 1$ Hz. Depending on these values, $\boldsymbol{B}^{\dagger}$ becomes 300×300 size. The one-minute signals are divided into 20 sub-frames of 300 samples each. These sub-frames are then multiplied with $\boldsymbol{B}^{\dagger}$ as in **(4.1)**. We have considered first 51 coefficients of all the 3 orders (zeroth, first, and second). These coefficients give us spectral information about frequencies 0-50 Hz with a separation of 1 Hz. As the signal is sampled at 100 Hz, from Nyquist theorem, the signal's frequencies beyond 50 Hz cannot be reproduced. Which means, the filters with central frequencies beyond 50 Hz does not give any prominent details. Taking 51 coefficients of all 3 orders will give us 153 coefficients in total. Each coefficient from every sub-frame is taken and averaged to get single value, thus we have 153 values for a one-minute signal. These values are log transformed and used as features for training. The use of logarithm as discussed in section 4.2 increased accuracy by about 0.5%. The confusion matrix corresponding to the model is shown in Fig. 6.1.

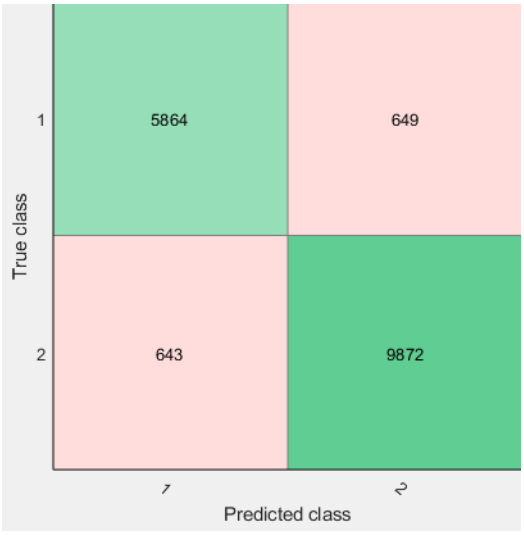

Fig. 6.1: Confusion matrix of results obtained (Class 1: apnea and Class 2: non-apnea)

The model is also 10-fold cross-validated as mentioned in chapter 5. The obtained accuracy is 92.41%, sensitivity is 90.11%, and specificity is 93.83%. Table 6.1 illustrates a comparison of the performance parameters obtained in previous works against our work.

Table 6.1: Performance comparison of different previous works.

Ref. No.	**Author(s)**	Accuracy(%)	Specificity(%)	Sensitivity(%)
[14]	Tripathy 2018	76.37	74.64	78.02
[28]	Chen et al, 2015b	82.07	80.24	83.23
[9]	Hassan 2015a	83.77	82.79	85.2
[2]	Varon et al. 2015	84.74	84.69	84.71
[3]	Nguyen et al. 2014	85.26	83.47	86.37
[29]	Hassan and Haque 2016	85.97	86.83	84.14
[30]	Song et al. 2016	86.2	88.4	82.6
[31]	Hassan 2016	87.33	90.72	81.99
[8]	Hassan and Haque 2017	88.88	91.49	87.58
[32]	Janbakshi et al. 2018	90.9	91.8	89.6
-	**Proposed Work**	**92.41**	**93.83**	**90.11**

The approach discussed in this work produces satisfying results with 92.41% accuracy, which is better than that of the previous works mentioned in Table 6.1.

Chapter 7

Conclusions and future scope

In our work, we make use of the digital Taylor-Fourier transform, which allows us to look at an ECG signal in a different perspective. The coefficients obtained contain more information about the signal than the standard time-domain analysis and are a very good measure to predict apnea and non-apnea. The high 10-fold cross-validation accuracy suggests that the model trained using these features can predict outcomes consistently with high reliability. In the biomedical domain, these numbers are quite significant and play a crucial role in deciding further treatment process. Also, the computational efficiency achieved due to the multi-frames processing nature of the transform shows that our method can save time, which is an important factor when it comes to biomedical applications.

Future work may include tasks like creating a user-friendly graphical user interface (GUI) of the entire process mentioned in the report which can help doctors in real-time analysis. New and better features which can improve the accuracy of the model can be developed. Proper emphasis should also be placed on the machine learning algorithms to get a good classifier which could produce better results. The suggested method in this work can be studied in the future for analysis and classification of other biomedical signals.

References

[1] A. A. Sleep Medicine Task Force and others, "Sleep-related breathing disorders in adults: recommendations for syndrome definition and measurement techniques in clinical research," *Sleep,* vol. 22, pp. 667-689, 1999.

[2] C. Varon, A. Caicedo, D. Testelmans, B. B. and V. H. S., "A Novel Algorithm for the Automatic Detection of Sleep Apnea From Single-Lead ECG," *IEEE Transactions on Biomedical Engineering,* vol. 62, no. 9, pp. 2269-2278, 2015.

[3] H. D. Nguyen, B. A. Wilkins, Q. Cheng and B. A. Benjamin, "An online sleep apnea detection method based on recurrence quantification analysis," *IEEE Journal of Biomedical and Health Informatics,* vol. 18, pp. 1285-1293, 2014.

[4] K. K. Motamedi, A. C. McClary and R. G. Amedee, "Obstructive sleep apnea: a growing problem," *The Ochsner Journal,* vol. 9, pp. 149-153, 2009.

[5] P. De Chazal, C. Heneghan, E. Sheridan, R. Reilly, P. Nolan and M. O'Malley, "Automated processing of the single-lead electrocardiogram for the detection of obstructive sleep apnoea," *IEEE Transactions on Biomedical Engineering,* vol. 50, pp. 686-696, 2003.

[6] A. Nishad, R. B. Pachori and U. R. Acharya, "Application of TQWT based filter-bank for sleep apnea screening using ECG signals," *Journal of Ambient Intelligence and Humanized Computing,* pp. 1-12, 2018.

[7] T. Penzel, J. McNames, P. De Chazal, B. Raymond, A. Murray and G. Moody, "Systematic comparison of different algorithms for apnoea detection based on electrocardiogram recordings," *Medical and Biological Engineering and Computing,* vol. 40, pp. 402-407, 2002.

[8] A. R. Hassan and M. A. Haque, "An expert system for automated identification of obstructive sleep apnea from single-lead ECG using random under sampling boosting," *Neurocomputing,* vol. 235, pp. 122-130, 2017.

[9] A. R. Hassan, "A comparative study of various classifiers for automated sleep apnea screening based on single-lead electrocardiogram," in *Electrical & Electronic Engineering (ICEEE), 2015 International Conference on*, 2015.

[10] L. Chen, X. Zhang and C. Song, "An automatic screening approach for obstructive sleep apnea diagnosis based on single-lead electrocardiogram," *IEEE Transactions on Automation Science and Engineering,* vol. 12, pp. 106-115, 2015.

[11] M. O. Mendez, A. M. Bianchi, M. Matteucci, S. Cerutti and T. Penzel, "Sleep apnea screening by autoregressive models from a single ECG lead," *IEEE Transactions on Biomedical Engineering,* vol. 56, pp. 2838-2850, 2009.

[12] T. S. Kumar and V. Kanhangad, "Gabor filter-based one-dimensional local phase descriptors for obstructive sleep apnea detection using single-lead ECG," *IEEE Sensors Letters,* vol. 2, pp. 1-4, 2018.

[13] A. H. Khandoker, M. Palaniswami and C. K. Karmakar, "Support vector machines for automated recognition of obstructive sleep apnea syndrome from ECG recordings," *IEEE Transactions on Information Technology in Biomedicine,* vol. 13, pp. 37-48, 2009.

[14] R. K. Tripathy, "Application of intrinsic band function technique for automated detection of sleep apnea using HRV and EDR signals," *Biocybernetics and Biomedical Engineering,* vol. 38, pp. 136-144, 2018.

[15] J. A. O Serna, "Dynamic phasor estimates for power system oscillations and transient detection," in *Power Engineering Society General Meeting, 2006. IEEE*, 2006.

[16] M. A. Platas-Garza and J. A. O Serna, "Dynamic harmonic analysis through Taylor--Fourier transform," *IEEE Transactions on Instrumentation and Measurement,* vol. 60, pp. 804-813, 2011.

[17] R. K. Tripathy, A. Z. Mendez, O. Serna, M. R. Arrieta Paternina, J. G. Arrieta, G. R. Naik and others, "Detection of Life Threatening Ventricular Arrhythmia using Digital Taylor Fourier Transform," *Frontiers in Physiology,* vol. 9, p. 722, 2018.

[18] A. L. Goldberger, L. A. N. Amaral, L. Glass, J. M. Hausdorff, P. C. Ivanov, R. G. Mark, J. E. Mietus, G. B. Moody, C.-K. Peng and H. E. Stanley, "PhysioBank, PhysioToolkit, and PhysioNet: components of a new research resource for complex physiologic signals," *Circulation,* vol. 101, pp. e215--e220, 2000.

[19] V. D. A. Corino, L. T. Mainardi, M. Stridh and L. Sornmo, "Improved Time--Frequency Analysis of Atrial Fibrillation Signals Using Spectral Modeling," *IEEE Transactions on Biomedical Engineering,* vol. 55, pp. 2723-2730, 2008.

[20] F. Zhang and Y. Yan, "Selective harmonic elimination PWM control scheme on a three-phase four-leg voltage source inverter," *IEEE Transactions on Power Electronics,* vol. 24, pp. 1682-1689, 2009.

[21] A. Kamitani, T. Takayama and S. Ikuno, "Axisymmetric simulation of inductive measurement method for critical current density in bulk HTS: relation between third harmonic voltage and coil current," *IEEE Transactions on Applied Superconductivity,* vol. 19, pp. 2901-2904, 2009.

[22] C. Liguori, A. Paolillo and A. Pignotti, "An intelligent FFT-analyzer with harmonic interference effect correction and uncertainty evaluation," in *Instrumentation and Measurement Technology Conference, 2003. IMTC'03. Proceedings of the 20th IEEE*, 2003.

[23] C. P. Steinmetz, "Complex quantities and their use in electrical engineering," in *Proceedings of the International Electrical Congress*, 1893.

[24] J. A. O Serna, "Taylor--Fourier analysis of blood pressure oscillometric waveforms," *IEEE Transactions on Instrumentation and Measurement,* vol. 62, pp. 2511-2518, 2013.

[25] C. Cortes and V. Vapnik, "Support-vector networks," *Machine learning,* vol. 20, pp. 273-297, 1995.

[26] R. Kohavi, "A study of cross-validation and bootstrap for accuracy estimation and model selection," in *IJCAI*, 1995.

[27] A. T. Azar and S. A. El-Said, "Performance analysis of support vector machines classifiers in breast cancer mammography recognition," *Neural Computing and Applications,* vol. 24, pp. 1163-1177, 2014.

[28] L. Chen, X. Zhang and H. Wang, "An obstructive sleep apnea detection approach using kernel density classification based on single-lead electrocardiogram," *Journal of Medical Systems,* vol. 39, p. 47, 2015.

[29] A. R. Hassan and M. A. Haque, "Computer-aided obstructive sleep apnea screening from single-lead electrocardiogram using statistical and spectral features and bootstrap aggregating," *Biocybernetics and Biomedical Engineering,* vol. 36, pp. 256-266, 2016.

[30] C. Song, K. Liu, X. Zhang, L. Chen and X. Xian, "An obstructive sleep apnea detection approach using a discriminative hidden Markov model from ECG signals," *IEEE Transactions on Biomedical Engineering,* vol. 63, pp. 1532-1542, 2016.

[31] A. R. Hassan, "Computer-aided obstructive sleep apnea detection using normal inverse Gaussian parameters and adaptive boosting," *Biomedical Signal Processing and Control,* vol. 29, pp. 22-30, 2016.

[32] P. Janbakhshi and M. B. Shamsollahi, "Sleep apnea detection from single-lead ECG using features based on ECG-derived respiration (EDR) signals," *IRBM,* vol. 39, pp. 206-218, 2018.